3-2005

Role for Akt3/Protein Kinase Bγ in Attainment of Normal Brain Size

Rachel M. Easton
Center for Neurodegenerative Disease Research

Han Cho
Dartmouth College

Kristin Roovers
Center for Neurodegenerative Disease Research

Diana W. Shineman
Institute on Aging

MOLECULAR AND CELLULAR BIOLOGY, Mar. 2005, p. 1869–1878 Vol. 25, No. 5
0270-7306/05/$08.00+0 doi:10.1128/MCB.25.5.1869–1878.2005

Role for Akt3/Protein Kinase Bγ in Attainment of Normal Brain Size

Rachael M. Easton,[1] Han Cho,[1,2] Kristin Roovers,[1] Diana W. Shineman,[3] Moshe Mizrahi,[4] Mark S. Forman,[3] Virginia M.-Y. Lee,[3] Matthias Szabolcs,[5] Ron de Jong,[6,7] Tilman Oltersdorf,[6] Thomas Ludwig,[8,9] Argiris Efstratiadis,[9,10] and Morris J. Birnbaum[1,4]*

Department of Medicine,[1] Center for Neurodegenerative Disease Research, Department of Pathology and Laboratory Medicine and Institute on Aging,[3] and Howard Hughes Medical Institute,[4] University of Pennsylvania School of Medicine, Philadelphia, Pennsylvania; Department of Genetics, Dartmouth Medical School, Hanover, New Hampshire[2]; Departments of Pathology,[5] Anatomy and Cell Biology,[8] and Genetics and Development[10] and Institute for Cancer Genetics,[9] Columbia University, New York, New York; and IDUN Pharmaceuticals, Inc.,[6] and Syrrx, Inc.,[7] San Diego, California

Received 23 September 2004/Returned for modification 6 November 2004/Accepted 5 December 2004

Studies of *Drosophila* and mammals have revealed the importance of insulin signaling through phosphatidylinositol 3-kinase and the serine/threonine kinase Akt/protein kinase B for the regulation of cell, organ, and organismal growth. In mammals, three highly conserved proteins, Akt1, Akt2, and Akt3, comprise the Akt family, of which the first two are required for normal growth and metabolism, respectively. Here we address the function of Akt3. Like Akt1, Akt3 is not required for the maintenance of normal carbohydrate metabolism but is essential for the attainment of normal organ size. However, in contrast to *Akt1*$^{-/-}$ mice, which display a proportional decrease in the sizes of all organs, *Akt3*$^{-/-}$ mice present a selective 20% decrease in brain size. Moreover, although Akt1- and Akt3-deficient brains are reduced in size to approximately the same degree, the absence of Akt1 leads to a reduction in cell number, whereas the lack of Akt3 results in smaller and fewer cells. Finally, mammalian target of rapamycin signaling is attenuated in the brains of *Akt3*$^{-/-}$ but not *Akt1*$^{-/-}$ mice, suggesting that differential regulation of this pathway contributes to an isoform-specific regulation of cell growth.

While complex organisms grow toward determinate final sizes, there must be precise regulation within each tissue as well as coordination among organs to reach these final sizes (18, 24). The regulation of both cell number and size contributes to the establishment of organ size, whereas cell number appears to be predominant in determining differences between species. Several factors, including circulating hormones and metabolites as well as cell-autonomous signaling cascades, control these processes (31). One of the key extracellular effectors determining organismal size is insulin-like growth factor 1 (IGF1). As demonstrated by genetic studies with mice, IGF1 is required for normal embryonic and postnatal growth (4, 43, 44, 59). In addition, IGF1 controls the sizes of individual organs (43, 59). For example, normal brain growth requires IGF1 (6, 43), as IGF1-deficient brains are reduced in size secondary to a decrease in both cell number and cell size (6, 15). Similarly, humans with IGF1 deficiency display severe growth retardation and suffer from mental retardation (75).

In addition to extracellular factors, the intracellular signaling pathways determining growth are being uncovered. IGF1 acts through the type 1 IGF receptor to modulate an evolutionarily conserved pathway of molecules involved in the regulation of growth and metabolism (38, 53). For many hormones, including IGF1 and insulin, binding to a receptor stimulates its protein tyrosine kinase activity, leading to the phosphorylation of scaffold proteins of the insulin receptor substrate (IRS) family. IRS proteins assemble complexes that include a number of potential signaling proteins, of which the lipid kinase phosphatidylinositol 3-kinase (PI3K) appears to be the most critical for the maintenance of cell size and proliferation (10). PI3K catalyzes the generation of phosphatidylinositol 3,4,5-trisphosphate (PIP_3), which binds to several signaling molecules, in most cases via a canonical pleckstrin homology domain. One of these proteins is the phosphoinositide-dependent kinase 1, which, in cooperation with the poorly defined phosphoinositide-dependent kinase 2, activates Akt/protein kinase B (Akt/PKB) by phosphorylation at two critical residues (8). The lipid phosphatase PTEN negatively regulates this pathway by converting PIP_3 to phosphatidylinositol 4,5-bisphosphate (PIP_2). There is now evidence that the IRS/PI3K/Akt pathway is involved in the control of organ size in several model systems (28, 67). Initially, this pathway was established in the fruit fly *Drosophila melanogaster*, but it is now clear that it is also operational in mammals (7, 12, 50, 56, 71). Tissue-specific activation of this pathway, either by the overexpression of active PI3K or Akt or by a deletion of PTEN, results in an increase in the sizes of several organs, including the heart (19, 48, 64–66), the endocrine pancreas (70), the brain (2, 30, 37), lymphoid tissue (27), the prostate (45, 73), and mammary glands (23, 39). In all of these cases, the enlargement in organ size is due at least in part, and often exclusively, to an increase in cell size. When the activation of Akt occurs early in brain

* Corresponding author. Mailing address: University of Pennsylvania School of Medicine, Clinical Research Building 322, 415 Curie Blvd., Philadelphia, PA 19104. Phone: (215) 898-5001. Fax: (215) 573-9138. E-mail: birnbaum@mail.med.upenn.edu.

development, the brain's larger size is secondary to increases in cell size and number, with the latter resulting from the augmented proliferation of neuronal stem cells (30). However, the activation of this pathway later in development only affects cell size, and this increase requires the activation of a protein downstream of IRS/PI3K/Akt, the mammalian target of rapamycin (mTOR) (36, 37). Nutrients as well as growth factors regulate mTOR, which therefore serves as a critical element in the coordination of growth with the energy supply. mTOR activation results in the phosphorylation of downstream targets such as p70 S6 kinase and 4E-BP1, which regulate protein translation (55).

In contrast to overexpression studies, only a few reports have described the effects of reduction in the activity of the IRS/PI3K/Akt pathway in specific organs (51). In some cases, the deletion of a gene from all of the tissues of an animal results in a selective decrease in the size of a single organ. Examples of this include IRS2 and p70 S6 kinase, two proteins whose elimination leads to a reduction in the brain and the aggregate mass of the β cells of the pancreas, respectively (57, 63). Regarding the former, IRS2-deficient brains are 38% smaller than normal primarily due to decreased cell proliferation, as cell size and apoptosis are unaffected (63).

Understanding the requirement of Akt for the determination of compartment size in mammals is complicated by the existence of three isoforms encoded by independent genes, namely, Akt1/PKBα, Akt2/PKBβ, and Akt3/PKBγ. Despite their significant homology, Akt1 and Akt2 have distinct functions in the control of growth and metabolism, respectively (13, 16, 17). Akt1-deficient mice display impaired overall growth, whereas Akt2 null mice are insulin intolerant, demonstrating a diabetes-like syndrome (13, 16, 17). However, the function of Akt3 has not yet been assessed by the generation and characterization of *Akt3*$^{-/-}$ mice. The distribution of Akt3 mRNA is more limited than that of either Akt1 or Akt2 (76). Akt3 mRNA is most highly expressed in the brain and testes, but it is also detected in fat, lungs, and mammary glands (76). In human tissue, Northern blot analyses have demonstrated the highest expression in adult brains, lungs, and kidneys as well as in fetal hearts, livers, and brains (9). Thus, a critical question to be addressed is whether Akt3 is important for growth and/or metabolism and, if so, whether it exerts its effect on particular cell types.

We report here the generation of mice lacking Akt3, in which we have observed a selective reduction in brain size. Moreover, by comparing brains from *Akt3*$^{-/-}$ mice to brains from *Akt1*$^{-/-}$ mice, we demonstrate isoform-specific mechanisms for the regulation of brain size.

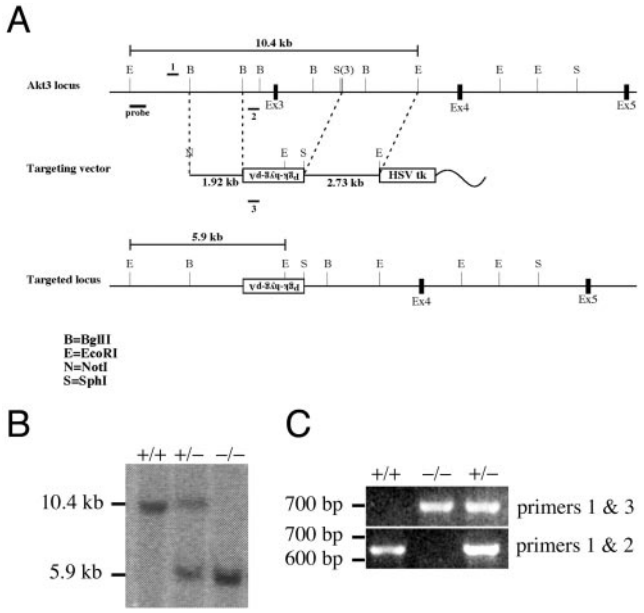

FIG. 1. Generation of Akt3-deficient mice. (A) Diagram of the Akt3 genomic locus and the targeting vector. The positions of the Southern probe (probe) and PCR primers (1, 2, and 3) are indicated. (B) Genomic DNAs isolated from wild-type (+/+), *Akt3* heterozygous (+/−), and *Akt3*-null (−/−) mice were digested with EcoRI and analyzed by Southern blotting. (C) PCR analysis of genomic DNAs from wild-type (+/+), *Akt3* heterozygous (+/−), and *Akt3*-null (−/−) mice. Primers 1 and 2 generate a 650-bp band from wild-type DNA, and primers 1 and 3 generate a 700-bp band from DNA with a targeted *Akt3* allele.

MATERIALS AND METHODS

Generation of Akt3-deficient mice. Using a mouse Akt3 cDNA probe, we isolated overlapping clones from a 129 mouse genomic library (Stratagene, La Jolla, Calif.). To introduce a null mutation, we deleted exon 3 (corresponding to nucleotides 209 to 320 of the mouse cDNA), which introduced a frame shift in the open reading frame and a truncation of the protein product.

The targeting construct (Fig. 1A) consisted of a 1.9-kb 5′ genomic fragment (NotI-BglII), a loxP-flanked phosphoglycerate kinase-hygromycin-poly(A) cassette in the opposite transcriptional orientation (SalI-BamHI fragment), and a 2.7-kb 3′ homology region (SphI-EcoRI). The 5′ homology fragment (NotI-BglII) and the loxP-flanked phosphoglycerate kinase-hygromycin-poly(A) cassette (SalI-BamHI) were cloned into pBKSKII that had been opened with NotI and SalI. The 3′ homology fragment (SphI-EcoRI) was subcloned into pSP73. The 5′ homology selection fragment was released with NotI and SalI and cloned with the 3′ homology fragment (XhoI-EcoRI) into a vector containing the herpes simplex virus thymidine kinase gene cassette (for negative selection). The targeting construct was linearized with NotI. Genomic DNAs from recombinant clones were digested with EcoRI and screened by Southern blot analysis. The probe recognized a 10.4-kb fragment in the wild-type allele and a 5.9-kb fragment in the targeted allele (Fig. 1B).

Mice were housed in a facility on a 12-h light-dark cycle with free access to food and water. All procedures were performed in accordance with the policies of the Institutional Animal Care and Use Committee at the University of Pennsylvania.

Mice were genotyped by PCR. Primers 1 (5′-GCA TCC ATC CTT GTT CAC GC) and 2 (5′-GGG AGA GAG AAG TGC CAT TGT ATT G) produced an ~650-bp band from DNAs of wild-type mice. Primers 1 and 3 (5′-GTG GGG TGG GAT TAG ATA AAT GC) produced an ~700-bp band from DNAs isolated from *Akt3*$^{-/-}$ mice (Fig. 1C).

An antibody to Akt3 was produced by use of a glutathione *S*-transferase fusion protein, with amino acids 1 to 147 of AKT3 as the antigen. Antisera were produced in rabbits and affinity purified by chromatography with the glutathione *S*-transferase fusion protein. Western blot analyses with this antibody did not detect any of the protein in brain extracts from Akt3 knockout animals (Fig. 2A).

Western blot analysis. Brains were homogenized in lysis buffer (50 mM Tris [pH 8], 250 mM NaCl, 2 mM EDTA, 1% IGEPAL, 200 mM NaF, 1 mM Na_3VO_4, complete protease inhibitor cocktail [Roche, Mannheim, Germany]). Homogenates were clarified by centrifugation, the supernatants were collected, and the protein concentration was determined by a bicinchoninic acid assay (BCA) (Pierce, Rockford, Ill.). For examinations of the phosphorylation of the ribosomal protein S6, 25 μg of protein was resolved by sodium dodecyl sulfate–15% polyacrylamide gel electrophoresis (SDS–15% PAGE). Blots were probed with anti-phospho-S6 (68) and anti-total S6 (Cell Signaling Technology, Beverly, Mass.). For the quantification of Akt isoforms, recombinant Akt1, Akt2, and Akt3 proteins were purchased from Upstate USA, Inc. (Charlottesville, Va.), and the concentration of each recombinant protein was determined by analysis

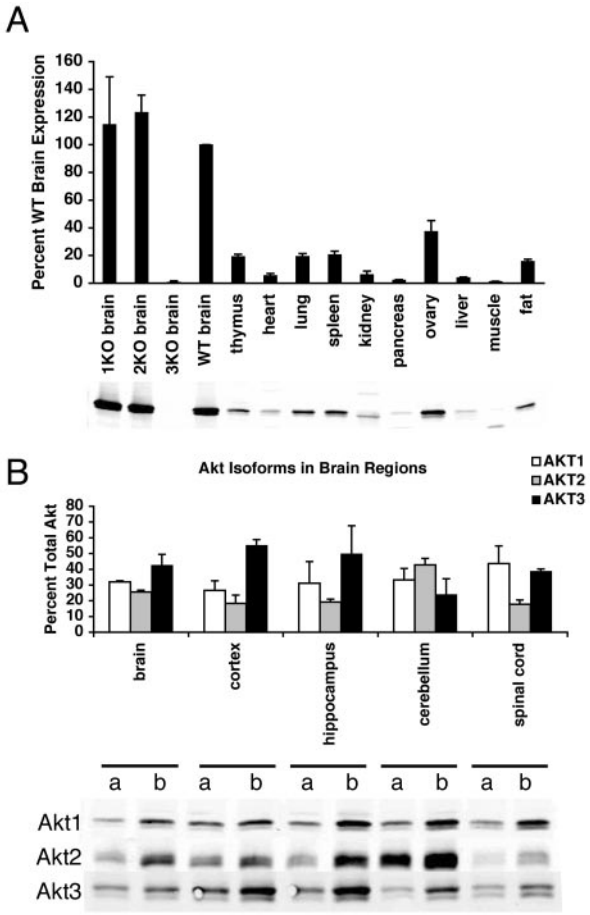

FIG. 2. Akt protein expression. (A) Tissues from three adult female wild-type mice were isolated for protein analysis. The amount of Akt3 protein in each tissue relative to the amount in the wild-type brain is depicted, and a representative Western blot is shown. Data for brains isolated from adult Akt1 (1KO)-, Akt2 (2KO)-, and Akt3 (3KO)-deficient mice are shown for comparison. The graph represents means ± SD for three blots. (B) Brains were dissected from three adult wild-type C57BL/6 mice, and the cortices, hippocampusi, and cerebella were isolated and homogenized for Akt protein measurements. Two dilutions (10 μg [a] and 20 μg [b]) from each sample were subjected to Western blot analysis. A standard curve of the recombinant protein for each isoform was used to quantify the amount of Akt in the lysate (as detailed in Materials and Methods). The mean amounts of protein in the two dilutions and the standard deviations are depicted by the bar graph, and a representative Western blot is shown below.

of a Coomassie blue-stained gel by use of the Odyssey system (LI-COR Biosciences, Lincoln, Nebr.) and a bovine serum albumin standard. A standard curve for each recombinant Akt protein and dilutions of total brain lysates were resolved by SDS–10% PAGE, transferred to nitrocellulose, and probed with isoform-specific antibodies (for Akt1 [Upstate USA, Inc.], Akt2 [68], and Akt3 [described above]). Brain lysates from each isoform-specific knockout animal were also included on the blot to ensure the specificities of the antibodies. Secondary antibodies were labeled with IR Dye 800 (Rockland Immunochemicals, Inc., Gilbertsville, Pa.) for quantification by the Odyssey system. The total amount of Akt protein was determined as the sum of the amounts of the individual isoforms, and the amount of each isoform was expressed as a percentage of the total amount of Akt protein.

Myelin assay. The myelin content in Akt3-deficient brains was measured as described by Cheng et al. (14). Briefly, brains from control and mutant mice were homogenized in 0.32 M sucrose. The brain homogenates were layered over an equal volume of 0.85 M sucrose and centrifuged at 75,000 × *g* for 30 min. Myelin was collected from the interface, osmotically shocked with water on ice for 30 min, and then sedimented by centrifugation at 12,000 × *g* for 20 min. The precipitate was resuspended in 10 mM Tris-HCl (pH 8.0)–1 mM EDTA, and the protein concentration was determined by a BCA protein assay.

Metabolic analysis. For glucose tolerance tests, glucose (1 g/kg of body weight) was administered by intraperitoneal injection to fasted conscious mice, and glucose concentrations were determined by use of a glucometer (Glucometer Elite XL; Bayer, Tarrytown, N.Y.) from whole blood collected from transversely sectioned tails. For insulin tolerance tests, porcine insulin (1 U/kg) was administered by intraperitoneal injection to fasted conscious mice, and glucose concentrations were determined by use of a glucometer from whole blood collected from transversely sectioned tails. Insulin and free fatty acid concentrations were measured as previously described, and insulin assays were performed by the Radioimmunoassay Core Facility at the Penn Center for Diabetes (17). A NEFA C kit (Wako Chemicals USA, Inc., Richmond, Va.) was used to determine free fatty acid levels.

DNA and protein content. For analyses of DNA and protein content, organs dissected from age-matched mutant and control animals were weighed and then homogenized in TNE buffer (10 mM Tris base, 10 mM EDTA, 200 mM NaCl, pH 7.4). An aliquot of each sample was diluted in TNE buffer containing 0.1 μg of Hoechst 33258/ml for measurement of the DNA content by use of a TD-700 fluorometer (Turner Designs, Sunnydale, Calif.) at an excitation wavelength of 365 nm and an emission wavelength of 460 nm. A standard curve using calf thymus DNA was used to calibrate the fluorometer. NP-40 (Sigma, St. Louis, Mo.) was added to the remaining brain homogenate to a final concentration of 1%, and the lysate was clarified by centrifugation at 16,000 × *g* at 4°C. The protein concentration of the supernatant was determined by a BCA protein assay. Data are expressed as percentages of the mean wild-type value, presented as means ± standard deviations (SD) for one experiment with littermate controls. Experiments were repeated at least three times.

Measurements of cardiomyocyte size. Hearts dissected from age- and sex-matched mutant and wild-type animals were fixed overnight in 10% neutral buffered formalin (NBF) (Sigma). After fixation, hearts were cut sagittally, embedded in paraffin, and sectioned. Five-micrometer sections were deparaffinized, stained with fluorescein isothiocyanate (FITC)-conjugated wheat germ agglutinin (Vector Laboratories Inc., Burlingame, Calif.), counterstained with propidium iodide, and then analyzed by microscopy with a Nikon Eclipse TE300 microscope (34). Two to eight 20× fields were analyzed per animal. The myocyte cross-sectional area was quantified by using the FITC-demarcated outline of the cell and Metamorph software (Universal Imaging Corporation, Downingtown, Pa.).

Analysis of cell density. Animals were anesthetized with pentobarbital and then perfused with phosphate-buffered saline containing 10 U of heparin/ml followed by 10% NBF. Brains were dissected, fixed overnight in 10% NBF, and transferred to 50 mM Tris–150 mM NaCl, pH 7.6, prior to being processed and embedded in paraffin. Six-micrometer sections were cut by use of a rotary microtome. Every other section was stained with cresyl violet. Sections were matched by the use of anatomic landmarks and a mouse brain atlas. Sections between 0.14 and 0.21 mm anterior to the bregma were deparaffinized and stained with 10 μg of Hoechst 33258/ml (Sigma). Quantification of the number of nuclei per defined area of motor cortex was performed with the Metamorph image analysis suite, and the mean cell area was expressed as the field area per number of cells. Three areas per slide were evaluated. Four to seven slides were evaluated per animal. Micrographs of motor cortexes were obtained with a cooled charge-coupled device camera (Princeton Instruments).

Livers isolated from Akt1- and Akt3-null mice were fixed in 10% NBF overnight, rinsed in phosphate-buffered saline, and then embedded in paraffin. Six-micrometer sections were cut by use of a rotary microtome. Sections were deparaffinized and stained with Hoechst 33258. The density was measured and the mean cell area was calculated as described above.

Statistical analysis. For comparisons between mutant and wild-type groups, Student's two-tailed *t* test was utilized and significant *P* values are indicated. The representative experiments shown were repeated at least three times.

RESULTS

Akt3 expression and generation of Akt3-deficient mice. Although the phenotypes of mice deficient in Akt1 and Akt2 are now well established, little is known about the role of Akt3 in mammals. For this reason, we generated mice in which the

expression of the *Akt3* gene was eliminated by standard targeting in embryonic stem cells (Fig. 1). As a consequence of this mutation, the Akt3 protein was undetectable in brains of knockout animals (Fig. 2A). *Akt3* nullizygous animals were born at a Mendelian frequency and did not exhibit any overt abnormalities for at least 1 year.

To search for potential phenotypic consequences of the Akt3 elimination that were not immediately obvious, we reevaluated the tissue distributions of Akt isoforms in the adult mouse, keeping in mind that mRNA and protein levels are not always in correlation, as, for example, in the case of Akt1 (76). Of all the mouse tissues examined, Akt3 expression was highest in the brain, which was consistent with the mRNA expression pattern (Fig. 2A). However, when we compared relative levels of mRNA and protein in different organs, protein expression, unlike mRNA expression, was observed in the heart, ovaries, and spleen (76).

To evaluate the relative expression of each of the Akt proteins in the brain, we developed an assay using isoform-specific antibodies and recombinant protein standards to quantify the absolute amounts of Akt1, -2, and -3. In adult brains, Akt3 was the predominant isoform, representing about one-half of the total Akt protein, whereas Akt1 accounted for approximately 30% of the total and Akt2 made up the rest (Fig. 2B). In postnatal day 1 brains, Akt1 was more abundant, accounting for 47% of the total Akt protein, whereas the relative levels of Akt2 and Akt3 were 14 and 39%, respectively (data not shown). Akt3 was present in all regions of the adult mouse brain and was the predominant isoform in the cortex and hippocampus. On the other hand, Akt2 was the most expressed isoform in the cerebellum, whereas Akt1 was the major isoform in the spinal cord (Fig. 2B).

Regulation of brain size by Akt3. Considering that Akt is required for the attainment of normal organ and organismal size in *D. melanogaster* and mice (13, 17, 61, 71) and that Akt3 is highly expressed in the mouse brain, we measured the brain weights of mutants lacking Akt3. Akt3-deficient mice demonstrated a reduction in brain size, as brains from adult nullizygotes were 25% smaller than those of their wild-type littermates, expressed either in absolute terms (349 ± 14.0 mg versus 464 ± 11.7 mg; $N = 6$ or 7; $P < 0.001$) (Fig. 3A and B) or as a ratio to body weight (Table 1). However, mouse size was unaffected by the Akt3 deficiency (Fig. 3C and D), and all organs examined other than the brain were normally sized (Table 2). Even the testes, which, like ovaries, had the second highest level of Akt3 protein expression, were normal in size in Akt3-deficient male mice (data not shown). Thus, the reduction in organ size in *Akt3*$^{-/-}$ mice was specific to the brain and was not proportional to body size (Table 2). This abnormality was present at birth, with postnatal day 1 mice displaying a 15% reduction in brain size compared to wild-type mice (68 ± 7.7 mg versus 80 ± 7.5 mg; $N = 13$ to 24; $P < 0.00$), despite their normal body size (1.4 ± 0.14 g for *Akt3*$^{+/+}$ animals versus 1.4 ± 0.17 g for *Akt3*$^{-/-}$ animals; $N = 13$ to 24) (Table 1). The relative reduction in brain size compared to the wild type continued to increase during the first 3 weeks of life, reaching the same degree as that seen in adults by the end of the third week (394 ± 19.1 mg for *Akt3*$^{+/+}$ animals versus 302 ± 21.7 mg for *Akt3*$^{-/-}$ animals; $N = 4$ or 5; $P < 0.01$).

To obtain a more quantitative estimate of the relationship between brain size and body weight, we performed an allometric analysis. Thus, we plotted the corresponding weight values for wild-type and Akt3 knockout mice as a logarithmic transformation of the scaling equation $y = ax^b$ and performed a linear regression analysis. This allowed us to determine the slope of the regression line, or allometric exponent b, which represents a formal quantitative measure of the relationship between x and y, in this case body weight and brain weight (Fig. 4). For wild-type mice, $b = 0.75$, which is in close approximation to that previously reported for mammals (47). In contrast, the value of b (0.61) for Akt3-deficient mice indicated that the brain size for a given body weight was significantly reduced.

Next, we considered possible effects of the Akt3 mutation on myelination, which begins during the first week of postnatal brain development and peaks within the third to fourth week of life (33, 52). IGF1 has been implicated in the control of this process, as its overexpression increases myelination (11). Moreover, IGF1-deficient brains have decreased myelination,

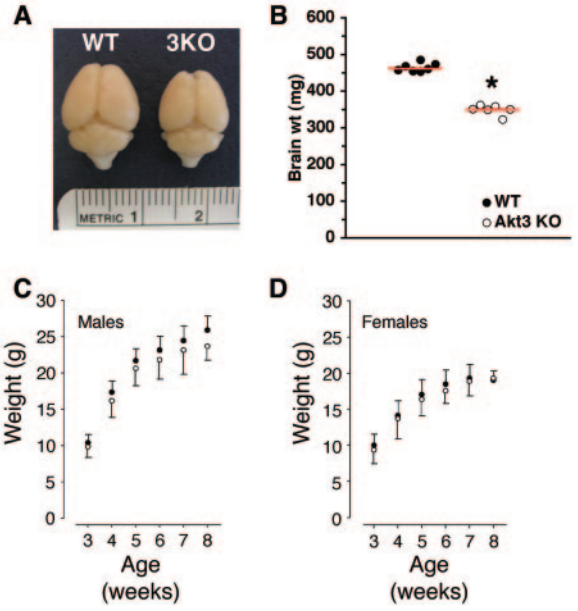

FIG. 3. Selective reduction of brain size in Akt3-deficient mice. (A) Brains were dissected from 30-week-old wild-type (WT) and Akt3-deficient (3KO) mice. (B) Plot of adult brain weights from Akt3 knockout mice and littermate controls ($N = 6$ or 7). The mean value is shown by a horizontal red bar. The asterisk indicates that $P < 0.001$ for wild-type versus Akt3-deficient brains. Male (C) and female (D) mice were weighed periodically during the first 8 weeks of life. Filled circles represent wild-type mice; open circles depict Akt3-deficient mice. Values are means ± standard errors of the means (SEM) ($N = 15$ to 20).

TABLE 1. Ratios of brain weights to body weights in wild-type and *Akt3*$^{-/-}$ mice

Mouse	Weight ratio[a] (mg/g) (*n*)		*P* value[b]
	Wild type	*Akt3*$^{-/-}$	
Postnatal day 1	55.9 ± 5.66 (13)	50.0 ± 6.37 (24)	<0.01
Adult	14.3 ± 1.41 (6)	11.6 ± 1.93 (7)	<0.05

[a] Data are means ± SD.
[b] Comparing wild-type and *Akt3*$^{-/-}$ mice.

TABLE 2. Comparison of organ-to-body-weight ratios for wild-type ($Akt3^{+/+}$) and Akt3-deficient ($Akt3^{-/-}$) mice[b]

Organ	Weight (mg)		% Body weight (relative to control)		P value[a]
	$Akt3^{+/+}$ ($n = 6$)	$Akt3^{-/-}$ ($n = 5$)	$Akt3^{+/+}$ ($n = 6$)	$Akt3^{-/-}$ ($n = 5$)	
Kidney	248 ± 17.7[b]	246 ± 38.0	100 ± 10.4	100 ± 15.1	NS
Liver	1,761 ± 56.4	1,550 ± 169.2	100 ± 7.1	93 ± 11.9	NS
Spleen	122 ± 29.1	141 ± 65.4	100 ± 24.4	100 ± 47.8	NS
Heart	213 ± 45.0	228 ± 22.3	100 ± 23.9	113 ± 17.5	NS
Thymus	40 ± 4.0	42 ± 1.1	100 ± 9.5	100 ± 19.2	NS
Brain	432 ± 23.0	338 ± 20.3	100 ± 9.1	82 ± 6.2	<0.01
Body	34 ± 1.9[c]	32 ± 3.0[c]			

[a] Comparing wild-type and $Akt3^{-/-}$ mice. NS, not significant ($P > 0.05$).
[b] Data are means ± SD.
[c] Body weights are given in grams.

which is probably proportional to the reduction in cell number (6, 14). The total myelin content was reduced by 20% in Akt3-deficient brains (3.8 ± 0.27 mg; $N = 7$) compared to wild-type brains (4.7 ± 0.32 mg; $P = 0.005$; $N = 4$), which was commensurate with the decrease in brain size. Thus, when the myelin content was corrected for the brain weight, there was no significant difference between brains from Akt3-deficient (10.7 ± 0.73 μg of myelin/mg of brain) and wild-type (9.8 ± 0.78 μg of myelin/mg of brain) mice. We concluded, therefore, that a reduction in myelin alone does not account for the decrease in brain size in Akt3 knockout animals.

In *Drosophila*, the Akt homolog Dakt1 regulates organ size primarily by the control of cell growth, although the cell number can also influence organ volume (29, 71). To clarify how Akt3 controls mammalian brain size, we measured the DNA and protein content in brains from Akt3-null mice. In the absence of polyploidy, the total DNA content reflects the cell number, whereas the protein-to-DNA ratio conveys information about cell size. For example, if an organ were smaller because the cell number was reduced, then the total DNA content would be decreased but the protein-to-DNA ratio would remain unchanged. If cell size alone were decreased, then the protein content would be reduced but the total DNA content would be unaffected, thereby producing a decrease in the protein-to-DNA ratio.

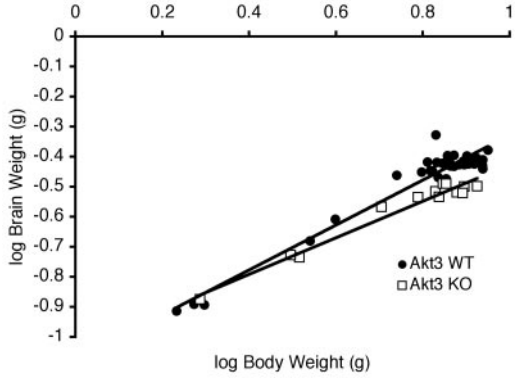

FIG. 4. Allometric plot. A log-log plot with first-order regression of the brain weights (BR) of wild-type and Akt3 knockout mice versus their corresponding body weights (BW) determined at postnatal days 3, 7, 12, 16, 20, 21, and 23 is shown. The results of the corresponding regression analyses were as follows: for wild-type mice, $BR = 0.08BW^{0.75}$ ($r = 0.97$); for Akt3 knockout mice, $BR = 0.09BW^{0.61}$ ($r = 0.98$).

In Akt3-deficient mice, the brain had a 13% decrease in total DNA content and an 11% reduction in the protein-to-DNA ratio (Table 3). This suggested that the 25% size reduction in the Akt3-deficient brain was secondary to both a decrease in cell number and a reduction in cell size. To obtain an independent measure of cell size, we measured the cell density in the adult cortex of Akt3-deficient brains and calculated the mean cell area. Using Hoechst 33258, we labeled nuclei in serial sections from matched regions of cerebral cortex and counted the number of nuclei in a defined area in both wild-type and knockout brains. In Akt3-deficient brains, the number of nuclei in the defined area was increased, indicative of a smaller mean cell area (Fig. 5). This reduction in cell size may be secondary to a change in the cell body size or to decreases in the number and size of dendrites. In neuronal cultures, inhibitory Akt constructs result in both diminished axon elongation and diminished soma size (46). In organs that were unaffected by the Akt3 deficiency, such as the liver and the heart (Table 2), which retained their normal sizes, no change in cell size was observed (data not shown), while the total DNA content and the protein-to-DNA ratio remained at wild-type levels (Table 3). We noted that the density of hepatocytes and the mean area of cardiomyocytes were normal in Akt3-deficient mice.

Analysis of metabolism in Akt3-deficient mice. In addition to regulating growth, the PI3K/Akt pathway is also required for normal metabolism. For example, Akt2 regulates glucose homeostasis, as mice deficient in this isoform are hyperinsulinemic and hyperglycemic (16, 29). Akt3 is expressed in cultured adipocytes and its activity is increased by insulin, raising the possibility that Akt3 is also important for the regulation of glucose or fat metabolism (5). Nevertheless, serum insulin, glucose, and free fatty acids were normal in Akt3-null mice (Table 4). In addition, adult Akt3-deficient mice exhibited glucose and insulin tolerance that was indistinguishable from that of wild-type mice (Fig. 6). Thus, we were unable to detect abnormalities in carbohydrate metabolism in $Akt3^{-/-}$ mice.

Comparison of Akt3 mutants to Akt1- and Akt2-null mice. Akt1-deficient mice exhibited a 14% reduction in brain size compared to littermate controls (383 ± 32.9 mg versus 446 ± 8.6 mg; $N = 5$; $P = 0.01$) that was proportional to the reduction in body size. An analogous maintenance of normal organ size

TABLE 3. DNA and protein levels in organs from Akt knockout mice[a]

Organ	Total DNA (% of wild type)				Protein/DNA ratio (% of wild type)			
	Akt1		Akt3		Akt1		Akt3	
	Wild-type	Knockout	Wild-type	Knockout	Wild-type	Knockout	Wild-type	Knockout
Brain	100 ± 7.9	79 ± 4.8[b]	100 ± 1.1	87 ± 1.3[c]	100 ± 8.3	123 ± 9.4	100 ± 2.6	89 ± 4.0[c]
Heart	100 ± 12.9	109 ± 20.3	100 ± 0.7	97 ± 1.0	100 ± 8.8	78 ± 11.8[c]	100 ± 4.2	106 ± 3.2
Liver	100 ± 1.5	75 ± 1.3[b]	100 ± 0.7	105 ± 3.0	100 ± 3.3	108 ± 3.2	100 ± 3.3	95 ± 5.1

[a] $N = 3$ to 5 for each group.
[b] $P < 0.05$ for wild-type versus knockout animals.
[c] $P \leq 0.01$ for wild-type versus knockout animals.

for body size was also observed for the livers and hearts of Akt1 nullizygotes (data not shown). *Akt2*-null mice displayed no change in brain size compared to control animals (431 ± 19.3 mg versus 439 ± 20.6 mg; N = 4).

Unlike Akt3, Akt1 was required for the size control of other organs, such as the heart and liver, in addition to the brain. In Akt1-deficient brains, the total DNA content was reduced by 21% and there was a trend towards an increased protein/DNA ratio that did not achieve statistical significance (Table 3). These data suggest that Akt1 is required mainly for the determination of the proper cell number. As performed with Akt3-deficient brains, we labeled nuclei in serial sections from matched regions of the cerebral cortex and counted the number of nuclei in a defined area in both wild-type and Akt1 knockout brains. We found no difference in the numbers of nuclei per area in Akt1-deficient cortices compared to wild-type controls (Fig. 7A to C). While Akt1 affected the cell number in the brain, Akt1-deficient hearts had a normal cell number, as indicated by an unchanged total DNA content compared to wild-type hearts (Table 3). However, hearts from $Akt1^{-/-}$ mice displayed a 21% reduction in the protein-to-DNA ratio, suggesting that the cells were smaller (Table 3). This was confirmed by direct measurements of myocyte cross-sectional areas by light microscopy (Fig. 7D to F). Akt1-deficient cardiomyocytes were 19% smaller than wild-type heart cells (202 ± 12.7 μm^2 versus 249 ± 13.6 μm^2; $N = 5$; $P < 0.01$) (Fig. 7D to F). The same result was obtained when the number of nuclei was counted in each field and when the mean cell size was computed as performed for brains (data not shown).

Unlike the heart, the Akt1-deficient liver revealed a normal protein-to-DNA ratio, suggesting an appropriate cell size, but had a 25% reduction in the total DNA content, which was representative of a decrease in cell number (Table 3). As described above for the heart and brain, liver sections from Akt1-deficient and Akt1 wild-type mice were stained with Hoechst 33258, and the numbers of nuclei were determined for defined fields. The cell density did not differ between Akt1 knockout and wild-type liver sections (1,745 ± 44.6 cells/mm^2 versus 1,755 ± 41.5 cells/mm^2; $N = 3$), indicating that there was no change in the mean cell area (473 ± 35.5 μm^2 for $Akt1^{-/-}$ animals versus 536 ± 43.5 μm^2 for $Akt1^{+/+}$ animals). Thus, livers from $Akt1^{-/-}$ mice were smaller due to an overall decrease in the number of cells.

Differential activation of downstream targets by Akt isoforms. One explanation for the distinct effects of Akt1 and Akt3 in the brain may be that the different isoforms of Akt regulate unique downstream targets. The mTOR-p70 S6 kinase pathway, which is downstream of Akt, regulates cell size (55) and is active during the period of brain growth throughout

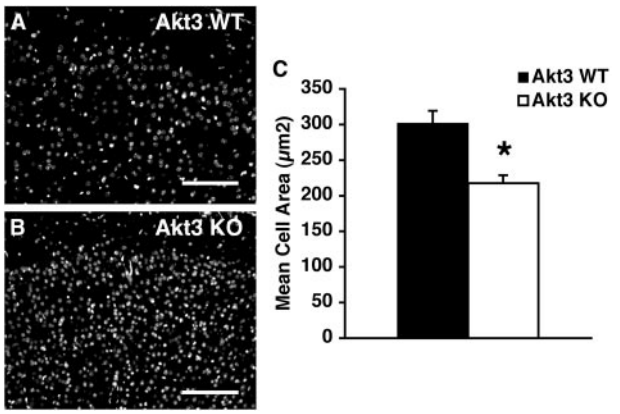

FIG. 5. Cell size in the Akt3-deficient brain. (A and B) Sections of cortex stained with Hoechst 33258. Bar = 100 μm. (C) Mean cell areas based on nuclear densities. *, $P < 0.001$ for Akt3 knockout (KO) versus wild-type (WT) brains.

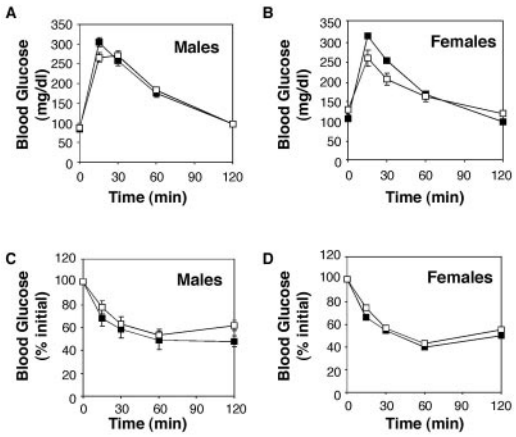

FIG. 6. Metabolism in Akt3-deficient mice. (A and B) Glucose tolerance tests were performed with male (A) and female (B) mice as described in Materials and Methods. Values represent means ± SEM ($N = 8$ to 10). Filled squares represent wild-type mice; open squares depict Akt3-deficient mice. (C and D) Insulin tolerance tests were performed with male (C) and female (D) mice as described in Materials and Methods. Values represent means ± SEM ($N = 8$ to 10). Filled squares represent wild-type mice; open squares depict Akt3-deficient mice.

TABLE 4. Circulating metabolites in Akt3 knockout mice

Metabolic parameter[a]	Value for males		Value for females	
	Wild-type	Knockout	Wild-type	Knockout
Fasting insulin (ng/ml)	0.363 ± 0.0214	0.399 ± 0.0601	0.365 ± 0.0394	0.427 ± 0.0539
Fasting glucose (mg/dl)	72 ± 1.6	79 ± 3.1	79 ± 5.9	87 ± 5.9
Fed glucose (mg/dl)	145 ± 5.6	159 ± 11.4	ND	ND
Fed FFA (mEq/liter)	0.25 ± 0.055	0.20 ± 0.035	0.20 ± 0.011	0.22 ± 0.032
Fasting FFA (mEq/liter)	1.11 ± 0.046	1.10 ± 0.112	0.98 ± 0.074	1.00 ± 0.062

[a] Data are means ± SD. $N = 7$ for each group. FFA, free fatty acids; ND, not done.

the first two postnatal weeks (69). mTOR is also required for the growth induced by PTEN activation (36). Therefore, we evaluated the phosphorylation of ribosomal protein S6, a downstream target of mTOR, in brains isolated from postnatal day 1 mice, in which p70 S6 kinase demonstrates peak activity (69). In Akt3 knockout brains, ribosomal protein S6 phosphorylation was decreased almost 50%. However, no reduction was observed in Akt1-null brains (Fig. 8). Similarly, the phosphorylation of p70 S6 kinase at serine 389 was reduced by 30% in Akt3-deficient brains, while no significant alteration was observed in Akt1 mutant brains (data not shown). Thus, Akt3 is required for the normal phosphorylation of p70 S6 kinase and its target, ribosomal protein S6, during postnatal brain growth.

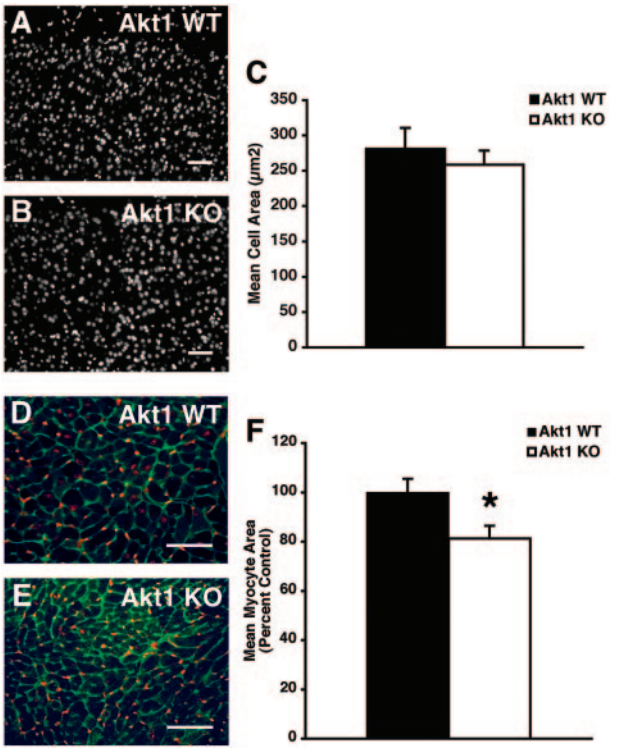

FIG. 7. Cell size in Akt1-deficient brains and hearts. (A and B) Sections of cortex stained with Hoechst 33258. Bar = 50 μm. (C) Mean cell areas based on nuclear densities. (D and E) Micrographs of sections of hearts from Akt1 knockout mice (E) and littermate controls (D) were stained with FITC-conjugated wheat germ agglutinin (green) and propidium iodide (red). (F) The mean cell area of cardiomyocytes is represented as a percentage of the mean wild-type control value. Values are means ± SD ($N = 3$). *, $P < 0.01$ for Akt1 knockout myocyte size versus wild-type control size.

DISCUSSION

Our analysis of the Akt3 null phenotype has provided the first evidence of a nonredundant function for this protein kinase in mammals. Similar to the closely related isoform Akt1, Akt3 does not appear to contribute significantly to the maintenance of normal metabolism but is critical for the attainment of normal organ size. However, in marked contrast to Akt1, Akt3 does not regulate organismal size but controls exclusively the mass of the mouse brain by influencing both cell size and number, most likely, at least in part, through the selective activation of downstream effectors in the mTOR pathway.

Now that experiments with fruit flies and mice have convincingly demonstrated a role for the PI3K/Akt pathway in the control of cell and compartment size, the question arises of how specificity is achieved given the large number of regulatory processes for which Akt appears to function as an essential intermediary (62). Although some of the previous studies that considered this issue relied on knockout strategies like ours, most reports have been based on overexpression studies of wild-type, constitutively active, or dominant-negative mutants (20, 22, 46, 66). We have reported previously that at least some of the specificity of Akt signaling, when growth versus metabolism is considered, is conferred by dissimilarities between Akt1 and Akt2 and that differences intrinsic to the Akt proteins contribute to selective signaling (3, 16, 17). The present study extends those observations by providing the unexpected

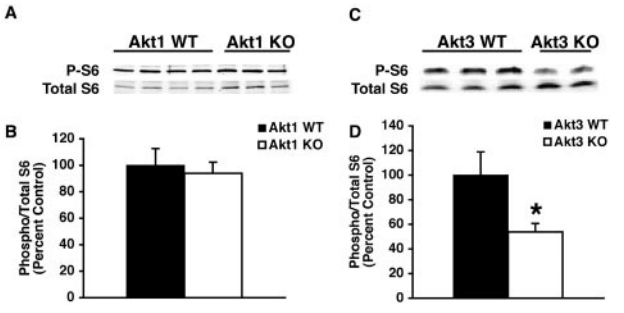

FIG. 8. Phosphorylation of ribosomal protein S6 in brains from Akt-deficient mice. (A and C) Lysates (25 μg) from postnatal day 1 brains were resolved by SDS-PAGE, transferred to a nitrocellulose membrane, and probed for phosphorylated ribosomal protein S6 (P-S6) or total S6 ribosomal protein as indicated. Each lane represents a lysate from an individual animal. (B and D) The intensities of phosphorylated ribosomal protein S6 from several experiments were normalized to that of the total S6 ribosomal protein and expressed as percentages of the mean wild-type value. The data shown are means ± SD ($N = 3$ to 6). *, $P < 0.01$ for Akt3 knockout versus wild-type littermates.

result that two Akt isoforms, Akt1 and Akt3, are both essential for normal growth control but that each functions in a distinct manner. Whereas Akt1 is important for global, organismal growth, the requirement for Akt3 is remarkably organ specific. It is likely that the mechanism is cell autonomous, because fibroblasts immortalized from *Akt1*-null mice also demonstrate a reduced size (4, 59; K. Roovers and M. J. Birnbaum, unpublished observations). Thus, growth control may be exerted by each Akt isoform operating as a signaling intermediate within the target cell. However, evidence that Akt1 and Akt3 have dissimilar signaling capabilities and do not simply function interchangeably is provided by the observation that the loss of each of the isoforms leads to a decreased brain size by distinct mechanisms, i.e, a reduction in only the cell number for $Akt1^{-/-}$ mice and in both cell size and number in $Akt3^{-/-}$ mutants. A probable explanation is that the activation of isoform-specific signaling pathways accounts for much of the difference, which is further modulated by external, developmentally regulated processes. For example, Akt3, but not Akt1, is required for appropriate ribosomal protein S6 phosphorylation during the postnatal period of brain growth (Fig. 8). However, these differences may be tissue specific, and Akt1 may be important for ribosomal protein S6 phosphorylation in the heart, where Akt1 controls cell size. In addition, selectivity in the ability of proximal signaling pathways to regulate Akt isoforms probably contributes to specificity. The elimination of the gene encoding IRS2, a scaffolding protein thought to lie upstream of Akt in a linear signaling pathway, results in an impairment of brain growth secondary to a decrease in neuronal proliferation (63). Interestingly, no change in cell survival or cell size was observed for IRS2-null brains, suggesting that IRS2 might preferentially regulate Akt1 in the brain, which would be surprising given the similarities between the roles of IRS2 and Akt2 in the control of peripheral metabolism (16, 29, 74). In addition, other induced mutations leading to organismal growth deficiencies, such as an IRS1 deficiency, cause a decrease in brain size and more closely resemble the phenotype of Akt1-null mice (1, 13, 17, 35, 76). Interestingly, in contrast to the case for $Akt1^{-/-}$ mice, for models based on a loss of IRS1, the diminution in brain size is not as severe as the reduction in body size (6, 63). This may occur because the IRS1-deficient animals are smaller than Akt1 knockout animals, and a commensurate reduction in brain size may not be compatible with life.

Previous studies have demonstrated that the activation of Akt by the deletion of PTEN affects brain size (30, 37). Since a PTEN deficiency modulates other targets in addition to Akt, it is important to demonstrate, as shown here, that this kinase is indeed a critical member of the pathway regulating normal brain growth. In mature neurons, the increase in brain size secondary to a targeted deletion of PTEN is a consequence of the increase in cell size and is dependent on the activation of mTOR (36). The deletion of PTEN at an earlier stage of neuronal development leads to both enlarged and more abundant cells (30). This suggests that the different phenotypes observed for $Akt1^{-/-}$ and $Akt3^{-/-}$ mice may be related to the stage of neuronal development at which each isoform is active, with Akt3 being more critical for the later periods of brain growth (21). The increased expression of the Akt3 protein in the adult brain is consistent with this hypothesis.

Several publications have reported experiments with brains and isolated neurons that implicate Akt in neuronal functions such as survival (20, 22, 32), process formation (54), cell growth (46), and synaptic plasticity (72). Unfortunately, these studies have relied on constitutively active or putative dominant-negative forms of Akt, which, in addition to their inherent problems of specificity, do not address Akt isoform selectivity. In this study, we confirmed the role of Akt in cell growth by using a loss-of-function strategy and further defined Akt1 and Akt3 as being the most important isoforms for this process in the brain. These genetic studies do not resolve, however, whether the reduction in cell number in the $Akt3^{-/-}$ brain is due to a defect in proliferation or survival. It has been argued that much of the macrocephaly in the brain-specific PTEN knockout is due to an expansion of central nervous system stem cells via increased proliferation (30). Akt has also been strongly implicated as a major regulator of the progression through the G_1 and G_2 phases of the cell cycle (41). Whether the lack of Akt1 and/or Akt3 decreases the cell number by affecting the proliferative capacity of stem cells will need to be evaluated in future studies. Interestingly, the microcephaly and macrocephaly of humans that are observed in IGF1-deficient patients and patients with the Lhermitte-Duclos PTEN deficiency syndrome, respectively, result in cognitive defects such as mental retardation (40, 75). This suggests a link between Akt and higher cerebral function that has not yet been studied in detail. Recently, a decrease in the Akt1 protein in the brain has been linked to schizophrenia (25). This is supported by the observation that a mutation in Akt1 leading to a decreased amount of protein increased the risk of schizophrenia, while the antipsychotic drug haloperidol was shown to activate Akt signaling (25). In rodents, the PI3K pathway has been implicated in memory formation (42, 49), which is often impaired in schizophrenic patients (26).

Finally, note that although the reduction in organ mass in Akt1-deficient mice was proportional to body size, the mechanism of this decrease depended on the tissue. Some indication that this is the case is provided by the observation that in $Akt1^{-/-}$ $Akt2^{-/-}$ mice, skeletal muscle atrophy is due to decreased myocyte size, whereas there is a reduced number of cells in the skin (58). These organ-specific differences in the modes of mass reduction may reflect the growth potential of particular organs. For example, the heart enlarges in the postnatal period exclusively through increases in cell size, whereas the liver maintains a proliferative capacity (60). It is perhaps for this reason that Akt1-deficient livers have decreased cell numbers, whereas Akt1-deficient hearts have smaller cells. Previous studies in which Akt activity was reduced in the heart have yielded contradictory results. The expression of a kinase-deficient Akt1 did not affect cardiac size, whereas a dominant-negative PI3K reduced the heart mass significantly (65, 66). This difference might be attributable to more attenuation in the total Akt activity produced by the mutant PI3K or to nonspecific actions of the dominant inhibitory form (19, 65). In this study, we have shown that Akt1 activity is required for the attainment of normal cardiomyocyte and heart size. This finding further serves to emphasize the remarkable capacity of the metazoan organism to coordinate the growth of individual organs and the critical role of Akt in this process.

ACKNOWLEDGMENTS

This work was partially funded by NIH grant R01 DK56886 to Morris Birnbaum and NCI grant P01 CA97403 (project 2) to Argiris Efstratiadis. Rachael Easton and Kristin Roovers were supported by NIH grant T32 DK7314 and by an American Heart Association fellowship, respectively. Services were also provided by the Radioimmunoassay Core of the Penn Diabetes Center (NIH grant DK19525) and the Morphology Core of the Center of Molecular Studies in Digestive and Liver Diseases (NIH grant DK50306).

REFERENCES

1. **Araki, E., M. A. Lipes, M. E. Patti, J. C. Bruning, B. Haag III, R. S. Johnson, and C. R. Kahn.** 1994. Alternative pathway of insulin signalling in mice with targeted disruption of the IRS-1 gene. Nature **372:**186–190.
2. **Backman, S. A., V. Stambolic, A. Suzuki, J. Haight, A. Elia, J. Pretorius, M. S. Tsao, P. Shannon, B. Bolon, G. O. Ivy, and T. W. Mak.** 2001. Deletion of Pten in mouse brain causes seizures, ataxia and defects in soma size resembling Lhermitte-Duclos disease. Nat. Genet. **29:**396–403.
3. **Bae, S. S., C. Han, J. Mu, and M. J. Birnbaum.** 2003. Isoform-specific regulation of insulin-dependent glucose uptake by Akt/protein kinase B. J. Biol. Chem. **278:**49530–49536.
4. **Baker, J., J. P. Liu, E. J. Robertson, and A. Efstratiadis.** 1993. Role of insulin-like growth factors in embryonic and postnatal growth. Cell **75:**73–82.
5. **Barthel, A., K. Nakatani, A. A. Dandekar, and R. A. Roth.** 1998. Protein kinase C modulates the insulin-stimulated increase in Akt1 and Akt3 activity in 3T3-L1 adipocytes. Biochem. Biophys. Res. Commun. **243:**509–513.
6. **Beck, K. D., L. Powell-Braxton, H. R. Widmer, J. Valverde, and F. Hefti.** 1995. Igf1 gene disruption results in reduced brain size, CNS hypomyelination, and loss of hippocampal granule and striatal parvalbumin-containing neurons. Neuron **14:**717–730.
7. **Bohni, R., J. Riesgo-Escovar, S. Oldham, W. Brogiolo, H. Stocker, B. F. Andruss, K. Beckingham, and E. Hafen.** 1999. Autonomous control of cell and organ size by CHICO, a Drosophila homolog of vertebrate IRS1-4. Cell **97:**865–875.
8. **Brazil, D. P., Z. Z. Yang, and B. A. Hemmings.** 2004. Advances in protein kinase B signalling: AKTion on multiple fronts. Trends Biochem. Sci. **29:** 233–242.
9. **Brodbeck, D., P. Cron, and B. A. Hemmings.** 1999. A human protein kinase Bgamma with regulatory phosphorylation sites in the activation loop and in the C-terminal hydrophobic domain. J. Biol. Chem. **274:**9133–9136.
10. **Cantley, L. C.** 2002. The phosphoinositide 3-kinase pathway. Science **296:** 1655–1657.
11. **Carson, M. J., R. R. Behringer, R. L. Brinster, and F. A. McMorris.** 1993. Insulin-like growth factor I increases brain growth and central nervous system myelination in transgenic mice. Neuron **10:**729–740.
12. **Chen, C., J. Jack, and R. S. Garofalo.** 1996. The Drosophila insulin receptor is required for normal growth. Endocrinology **137:**846–856.
13. **Chen, W. S., P. Z. Xu, K. Gottlob, M. L. Chen, K. Sokol, T. Shiyanova, I. Roninson, W. Weng, R. Suzuki, K. Tobe, T. Kadowaki, and N. Hay.** 2001. Growth retardation and increased apoptosis in mice with homozygous disruption of the Akt1 gene. Genes Dev. **15:**2203–2208.
14. **Cheng, C. M., G. Joncas, R. R. Reinhardt, R. Farrer, R. Quarles, J. Janssen, M. P. McDonald, J. N. Crawley, L. Powell-Braxton, and C. A. Bondy.** 1998. Biochemical and morphometric analyses show that myelination in the insulin-like growth factor 1 null brain is proportionate to its neuronal composition. J. Neurosci. **18:**5673–5681.
15. **Cheng, C. M., R. F. Mervis, S. L. Niu, N. Salem, Jr., L. A. Witters, V. Tseng, R. Reinhardt, and C. A. Bondy.** 2003. Insulin-like growth factor 1 is essential for normal dendritic growth. J. Neurosci. Res. **73:**1–9.
16. **Cho, H., J. Mu, J. K. Kim, J. L. Thorvaldsen, Q. Chu, E. B. Crenshaw III, K. H. Kaestner, M. S. Bartolomei, G. I. Shulman, and M. J. Birnbaum.** 2001. Insulin resistance and a diabetes mellitus-like syndrome in mice lacking the protein kinase Akt2 (PKB beta). Science **292:**1728–1731.
17. **Cho, H., J. L. Thorvaldsen, Q. Chu, F. Feng, and M. J. Birnbaum.** 2001. Akt1/PKBalpha is required for normal growth but dispensable for maintenance of glucose homeostasis in mice. J. Biol. Chem. **276:**38349–38352.
18. **Conlon, I., and M. Raff.** 1999. Size control in animal development. Cell **96:**235–244.
19. **Crackower, M. A., G. Y. Oudit, I. Kozieradzki, R. Sarao, H. Sun, T. Sasaki, E. Hirsch, A. Suzuki, T. Shioi, J. Irie-Sasaki, R. Sah, H. Y. Cheng, V. O. Rybin, G. Lembo, L. Fratta, A. J. Oliveira-dos-Santos, J. L. Benovic, C. R. Kahn, S. Izumo, S. F. Steinberg, M. P. Wymann, P. H. Backx, and J. M. Penninger.** 2002. Regulation of myocardial contractility and cell size by distinct PI3K-PTEN signaling pathways. Cell **110:**737–749.
20. **Crowder, R. J., and R. S. Freeman.** 1998. Phosphatidylinositol 3-kinase and Akt protein kinase are necessary and sufficient for the survival of nerve growth factor-dependent sympathetic neurons. J. Neurosci. **18:**2933–2943.
21. **Dobbing, J., and J. Sands.** 1979. Comparative aspects of the brain growth spurt. Early Hum. Dev. **3:**79–83.
22. **Dudek, H., S. R. Datta, T. F. Franke, M. J. Birnbaum, R. Yao, G. M. Cooper, R. A. Segal, D. R. Kaplan, and M. E. Greenberg.** 1997. Regulation of neuronal survival by the serine-threonine protein kinase Akt. Science **275:** 661–665.
23. **Dupont, J., J. P. Renou, M. Shani, L. Hennighausen, and D. LeRoith.** 2002. PTEN overexpression suppresses proliferation and differentiation and enhances apoptosis of the mouse mammary epithelium. J. Clin. Investig. **110:** 815–825.
24. **Efstratiadis, A.** 1998. Genetics of mouse growth. Int. J. Dev. Biol. **42:**955–976.
25. **Emamian, E. S., D. Hall, M. J. Birnbaum, M. Karayiorgou, and J. A. Gogos.** 2004. Convergent evidence for impaired AKT1-GSK3beta signaling in schizophrenia. Nat. Genet. **36:**131–137.
26. **Freedman, R.** 2003. Schizophrenia. N. Engl. J. Med. **349:**1738–1749.
27. **Fruman, D. A.** 2004. Phosphoinositide 3-kinase and its targets in B-cell and T-cell signaling. Curr. Opin. Immunol. **16:**314–320.
28. **Garofalo, R. S.** 2002. Genetic analysis of insulin signaling in Drosophila. Trends Endocrinol. Metab. **13:**156–162.
29. **Garofalo, R. S., S. J. Orena, K. Rafidi, A. J. Torchia, J. L. Stock, A. L. Hildebrandt, T. Coskran, S. C. Black, D. J. Brees, J. R. Wicks, J. D. McNeish, and K. G. Coleman.** 2003. Severe diabetes, age-dependent loss of adipose tissue, and mild growth deficiency in mice lacking Akt2/PKB beta. J. Clin. Investig. **112:**197–208.
30. **Groszer, M., R. Erickson, D. D. Scripture-Adams, R. Lesche, A. Trumpp, J. A. Zack, H. I. Kornblum, X. Liu, and H. Wu.** 2001. Negative regulation of neural stem/progenitor cell proliferation by the Pten tumor suppressor gene in vivo. Science **294:**2186–2189.
31. **Hafen, E., and H. Stocker.** 2003. How are the sizes of cells, organs, and bodies controlled? PLoS Biol. **1:**E86.
32. **Humbert, S., E. A. Bryson, F. P. Cordelieres, N. C. Connors, S. R. Datta, S. Finkbeiner, M. E. Greenberg, and F. Saudou.** 2002. The IGF-1/Akt pathway is neuroprotective in Huntington's disease and involves Huntington phosphorylation by Akt. Dev. Cell **2:**831–837.
33. **Jacobson, M.** 1991. Developmental neurobiology, 3rd ed., p. 95–142. Plenum Press, New York, N.Y.
34. **Jovanovic, S., A. J. Grantham, J. E. Tarara, J. C. Burnett, Jr., A. Jovanovic, and A. Terzic.** 1999. Increased number of cardiomyocytes in cross-sections from tachycardia-induced cardiomyopathic hearts. Int. J. Mol. Med. **3:**153–155.
35. **Kadowaki, T., H. Tamemoto, K. Tobe, Y. Terauchi, K. Ueki, Y. Kaburagi, T. Yamauchi, S. Satoh, H. Sekihara, S. Aizawa, and Y. Yazaki.** 1996. Insulin resistance and growth retardation in mice lacking insulin receptor substrate-1 and identification of insulin receptor substrate-2. Diabet. Med. **13:** S103–S108.
36. **Kwon, C. H., X. Zhu, J. Zhang, and S. J. Baker.** 2003. mTor is required for hypertrophy of Pten-deficient neuronal soma in vivo. Proc. Natl. Acad. Sci. USA **100:**12923–12928.
37. **Kwon, C. H., X. Zhu, J. Zhang, L. L. Knoop, R. Tharp, R. J. Smeyne, C. G. Eberhart, P. C. Burger, and S. J. Baker.** 2001. Pten regulates neuronal soma size: a mouse model of Lhermitte-Duclos disease. Nat. Genet. **29:**404–411.
38. **LeRoith, D., and C. T. Roberts, Jr.** 2003. The insulin-like growth factor system and cancer. Cancer Lett. **195:**127–137.
39. **Li, G., G. W. Robinson, R. Lesche, H. Martinez-Diaz, Z. Jiang, N. Rozengurt, K. U. Wagner, D. C. Wu, T. F. Lane, X. Liu, L. Hennighausen, and H. Wu.** 2002. Conditional loss of PTEN leads to precocious development and neoplasia in the mammary gland. Development **129:**4159–4170.
40. **Li, L., F. Liu, and A. H. Ross.** 2003. PTEN regulation of neural development and CNS stem cells. J. Cell Biochem. **88:**24–28.
41. **Liang, J., and J. M. Slingerland.** 2003. Multiple roles of the PI3K/PKB (Akt) pathway in cell cycle progression. Cell Cycle **2:**339–345.
42. **Lin, C. H., S. H. Yeh, K. T. Lu, T. H. Leu, W. C. Chang, and P. W. Gean.** 2001. A role for the PI-3 kinase signaling pathway in fear conditioning and synaptic plasticity in the amygdala. Neuron **31:**841–851.
43. **Liu, J. P., J. Baker, A. S. Perkins, E. J. Robertson, and A. Efstratiadis.** 1993. Mice carrying null mutations of the genes encoding insulin-like growth factor I (Igf-1) and type 1 IGF receptor (Igf1r). Cell **75:**59–72.
44. **Lupu, F., J. D. Terwilliger, K. Lee, G. V. Segre, and A. Efstratiadis.** 2001. Roles of growth hormone and insulin-like growth factor 1 in mouse postnatal growth. Dev. Biol. **229:**141–162.
45. **Majumder, P. K., J. J. Yeh, D. J. George, P. G. Febbo, J. Kum, Q. Xue, R. Bikoff, H. Ma, P. W. Kantoff, T. R. Golub, M. Loda, and W. R. Sellers.** 2003. Prostate intraepithelial neoplasia induced by prostate restricted Akt activation: the MPAKT model. Proc. Natl. Acad. Sci. USA **100:**7841–7846.
46. **Markus, A., J. Zhong, and W. D. Snider.** 2002. Raf and Akt mediate distinct aspects of sensory axon growth. Neuron **35:**65–76.
47. **Martin, R. D.** 1981. Relative brain size and basal metabolic rate in terrestrial vertebrates. Nature **293:**57–60.
48. **Matsui, T., L. Li, J. C. Wu, S. A. Cook, T. Nagoshi, M. H. Picard, R. Liao, and A. Rosenzweig.** 2002. Phenotypic spectrum caused by transgenic overexpression of activated Akt in the heart. J. Biol. Chem. **277:**22896–22901.
49. **Mizuno, M., K. Yamada, N. Takei, M. H. Tran, J. He, A. Nakajima, H. Nawa, and T. Nabeshima.** 2003. Phosphatidylinositol 3-kinase: a molecule mediating BDNF-dependent spatial memory formation. Mol. Psychiatry **8:**217–224.

50. **Montagne, J., M. J. Stewart, H. Stocker, E. Hafen, S. C. Kozma, and G. Thomas.** 1999. Drosophila S6 kinase: a regulator of cell size. Science **285:** 2126–2129.
51. **Mora, A., A. M. Davies, L. Bertrand, I. Sharif, G. R. Budas, S. Jovanovic, V. Mouton, C. R. Kahn, J. M. Lucocq, G. A. Gray, A. Jovanovic, and D. R. Alessi.** 2003. Deficiency of PDK1 in cardiac muscle results in heart failure and increased sensitivity to hypoxia. EMBO J. **22:**4666–4676.
52. **Morell, P. (ed.).** 1984. Myelin, 2nd ed. Plenum Press, New York, N.Y.
53. **Nakae, J., Y. Kido, and D. Accili.** 2001. Distinct and overlapping functions of insulin and IGF-I receptors. Endocr. Rev. **22:**818–835.
54. **Namikawa, K., M. Honma, K. Abe, M. Takeda, K. Mansur, T. Obata, A. Miwa, H. Okado, and H. Kiyama.** 2000. Akt/protein kinase B prevents injury-induced motoneuron death and accelerates axonal regeneration. J. Neurosci. **20:**2875–2886.
55. **Neufeld, T. P.** 2003. Body building: regulation of shape and size by PI3K/TOR signaling during development. Mech. Dev. **120:**1283–1296.
56. **Oldham, S., H. Stocker, M. Laffargue, F. Wittwer, M. Wymann, and E. Hafen.** 2002. The Drosophila insulin/IGF receptor controls growth and size by modulating PtdInsP(3) levels. Development **129:**4103–4109.
57. **Pende, M., S. C. Kozma, M. Jaquet, V. Oorschot, R. Burcelin, Y. Le Marchand-Brustel, J. Klumperman, B. Thorens, and G. Thomas.** 2000. Hypoinsulinaemia, glucose intolerance and diminished beta-cell size in S6K1-deficient mice. Nature **408:**994–997.
58. **Peng, X. D., P. Z. Xu, M. L. Chen, A. Hahn-Windgassen, J. Skeen, J. Jacobs, D. Sundararajan, W. S. Chen, S. E. Crawford, K. G. Coleman, and N. Hay.** 2003. Dwarfism, impaired skin development, skeletal muscle atrophy, delayed bone development, and impeded adipogenesis in mice lacking Akt1 and Akt2. Genes Dev. **17:**1352–1365.
59. **Powell-Braxton, L., P. Hollingshead, C. Warburton, M. Dowd, S. Pitts-Meek, D. Dalton, N. Gillett, and T. A. Stewart.** 1993. IGF-I is required for normal embryonic growth in mice. Genes Dev. **7:**2609–2617.
60. **Rakusan, K.** 1984. Cardiac growth, maturation and aging, p. 131–164. *In* R. Zak (ed.), Growth of the heart in health and disease. Raven Press, Ltd., New York, N.Y.
61. **Scanga, S. E., L. Ruel, R. C. Binari, B. Snow, V. Stambolic, D. Bouchard, M. Peters, B. Calvieri, T. W. Mak, J. R. Woodgett, and A. S. Manoukian.** 2000. The conserved PI3′K/PTEN/Akt signaling pathway regulates both cell size and survival in Drosophila. Oncogene **19:**3971–3977.
62. **Scheid, M. P., and J. R. Woodgett.** 2001. PKB/AKT: functional insights from genetic models. Nat. Rev. Mol. Cell Biol. **2:**760–768.
63. **Schubert, M., D. P. Brazil, D. J. Burks, J. A. Kushner, J. Ye, C. L. Flint, J. Farhang-Fallah, P. Dikkes, X. M. Warot, C. Rio, G. Corfas, and M. F. White.** 2003. Insulin receptor substrate-2 deficiency impairs brain growth and promotes tau phosphorylation. J. Neurosci. **23:**7084–7092.
64. **Schwartzbauer, G., and J. Robbins.** 2001. The tumor suppressor gene PTEN can regulate cardiac hypertrophy and survival. J. Biol. Chem. **276:**35786–35793.
65. **Shioi, T., P. M. Kang, P. S. Douglas, J. Hampe, C. M. Yballe, J. Lawitts, L. C. Cantley, and S. Izumo.** 2000. The conserved phosphoinositide 3-kinase pathway determines heart size in mice. EMBO J. **19:**2537–2548.
66. **Shioi, T., J. R. McMullen, P. M. Kang, P. S. Douglas, T. Obata, T. F. Franke, L. C. Cantley, and S. Izumo.** 2002. Akt/protein kinase B promotes organ growth in transgenic mice. Mol. Cell. Biol. **22:**2799–2809.
67. **Stocker, H., and E. Hafen.** 2000. Genetic control of cell size. Curr. Opin. Genet. Dev. **10:**529–535.
68. **Summers, S. A., L. Lipfert, and M. J. Birnbaum.** 1998. Polyoma middle T antigen activates the Ser/Thr kinase Akt in a PI3-kinase-dependent manner. Biochem. Biophys. Res. Commun. **246:**76–81.
69. **Tsuji, R., M. Guizzetti, and L. G. Costa.** 2003. In vivo ethanol decreases phosphorylated MAPK and p70S6 kinase in the developing rat brain. Neuroreport **14:**1395–1399.
70. **Tuttle, R. L., N. S. Gill, W. Pugh, J. P. Lee, B. Koeberlein, E. E. Furth, K. S. Polonsky, A. Naji, and M. J. Birnbaum.** 2001. Regulation of pancreatic beta-cell growth and survival by the serine/threonine protein kinase Akt1/PKBalpha. Nat. Med. **7:**1133–1137.
71. **Verdu, J., M. A. Buratovich, E. L. Wilder, and M. J. Birnbaum.** 1999. Cell-autonomous regulation of cell and organ growth in Drosophila by Akt/PKB. Nat. Cell Biol. **1:**500–506.
72. **Wang, Q., L. Liu, L. Pei, W. Ju, G. Ahmadian, J. Lu, Y. Wang, F. Liu, and Y. T. Wang.** 2003. Control of synaptic strength, a novel function of Akt. Neuron **38:**915–928.
73. **Wang, S., J. Gao, Q. Lei, N. Rozengurt, C. Pritchard, J. Jiao, G. V. Thomas, G. Li, P. Roy-Burman, P. S. Nelson, X. Liu, and H. Wu.** 2003. Prostate-specific deletion of the murine Pten tumor suppressor gene leads to metastatic prostate cancer. Cancer Cell **4:**209–221.
74. **Withers, D. J., J. S. Gutierrez, H. Towery, D. J. Burks, J. M. Ren, S. Previs, Y. Zhang, D. Bernal, S. Pons, G. I. Shulman, S. Bonner-Weir, and M. F. White.** 1998. Disruption of IRS-2 causes type 2 diabetes in mice. Nature **391:**900–904.
75. **Woods, K. A., C. Camacho-Hubner, D. Barter, A. J. Clark, and M. O. Savage.** 1997. Insulin-like growth factor I gene deletion causing intrauterine growth retardation and severe short stature. Acta Paediatr. **423**(Suppl.)**:**39–45.
76. **Yang, Z. Z., O. Tschopp, M. Hemmings-Mieszczak, J. Feng, D. Brodbeck, E. Perentes, and B. A. Hemmings.** 2003. Protein kinase B alpha/Akt1 regulates placental development and fetal growth. J. Biol. Chem. **278:**32124–32131.